NANO LETTERS

2009
Vol. 9, No. 8
2909-2913

Surface Phonon Polaritons Mediated Energy Transfer between Nanoscale Gaps

Sheng Shen,[†] Arvind Narayanaswamy,[*,‡] and Gang Chen[*,†]

Department of Mechanical Engineering, Massachusetts Institute of Technology, Cambridge, Massachusetts 02139, Department of Mechanical Engineering, Columbia University, New York, New York 10027

Received April 16, 2009; Revised Manuscript Received June 18, 2009

ABSTRACT

Surface phonon polaritons are electromagnetic waves that propagate along the interfaces of polar dielectrics and exhibit a large local-field enhancement near the interfaces at infrared frequencies. Theoretical calculations show that such surface waves can lead to breakdown of the Planck's blackbody radiation law in the near field. Here, we experimentally demonstrate that surface phonon polaritons dramatically enhance energy transfer between two surfaces at small gaps by measuring radiation heat transfer between a microsphere and a flat surface down to 30 nm separation. The corresponding heat transfer coefficients at nanoscale gaps are 3 orders of magnitude larger than that of the blackbody radiation limit. The high energy flux can be exploited to develop new radiative cooling and thermophotovoltaic technologies.

Although Planck's blackbody radiation is often considered as the maximum of heat radiation between two surfaces, Planck himself recognized that the law bearing his name is not valid when the characteristic length scales are comparable to the wavelength of thermal radiation.[1] The theoretical foundation of near-field radiation was established based on fluctuational electrodynamics theory[2,3] and has been employed to study near-field radiation between the surfaces of metals,[3] dielectrics[4−6] and semiconductors.[7] In particular, theory has predicted that near-field radiation between polar dielectric materials (SiO_2, SiC, BN, etc.), which support resonant surface phonon polaritons, is dominated by the surface phonon-polariton contribution and can be enhanced by several orders of magnitude beyond the Planck's blackbody radiation limit.[4] So far, however, such significant enhancement of energy transfer mediated by surface phonon polaritons has not been experimentally demonstrated. In this letter, we clearly show this enhancement by measuring near-field thermal radiation between a glass sphere and different substrate materials with a sensitive bimaterial atomic force microscope cantilever.[8,9]

Surface phonon-polariton, which originates from the resonant coupling between the electromagnetic field and optical phonons in polar dielectrics, is an infrared counterpart of surface plasmon-polariton that usually exists on metal surfaces in the visible and ultraviolet range. In both cases, these surface waves share the following properties: they are modes of the system that can be resonantly excited; and they are characterized by large energy densities at the interface, which decay rapidly with distance from the surface.[10,11] Figure 1A shows the calculated local density of states (LDOS)[12] in vacuum at 50 nm above an interface between vacuum and three different materials considered in our experiments. Silicon dioxide (glass) is a polar dielectric material that can support surface phonon polaritons, although compared to crystalline polar materials such as SiC, the resonance is broadened due to stronger damping in amorphous materials. The large peaks in LDOS are observed near the surface of polar materials at certain wavelengths ($\lambda \approx 8.5\ \mu$m and $\lambda \approx 20.3\ \mu$m for glass) that correspond to surface phonon-polariton resonances. Silicon and gold surfaces, however, do not exhibit any strong resonant excitation peaks in the spectral region under consideration. These surface waves on SiO_2 surface decay rapidly away from the interface. Hence, despite the high energy density near the interface (Figure 1A), these surface waves do not lead to far-field emission. When another surface is brought close by, the surface waves can tunnel from one side to the other, contributing significantly to heat transfer. Figure 1B,C shows, respectively, the spectral and total radiative heat transfer coefficients defined as the net radiative flux (per unit wavelength interval for spectral heat transfer coefficients) divided by the temperature difference between two parallel plates made of different material combinations (SiO_2-SiO_2,

* To whom correspondence should be addressed. (G.C.) Phone: 617-253-0006. Fax: 617-258-5802. E-mail: gchen2@mit.edu. (A.N.) Phone: 212-854-0303. E-mail: arvind.narayanaswamy@columbia.edu.
† Massachusetts Institute of Technology.
‡ Columbia University.

10.1021/nl901208v CCC: $40.75
Published on Web 07/02/2009

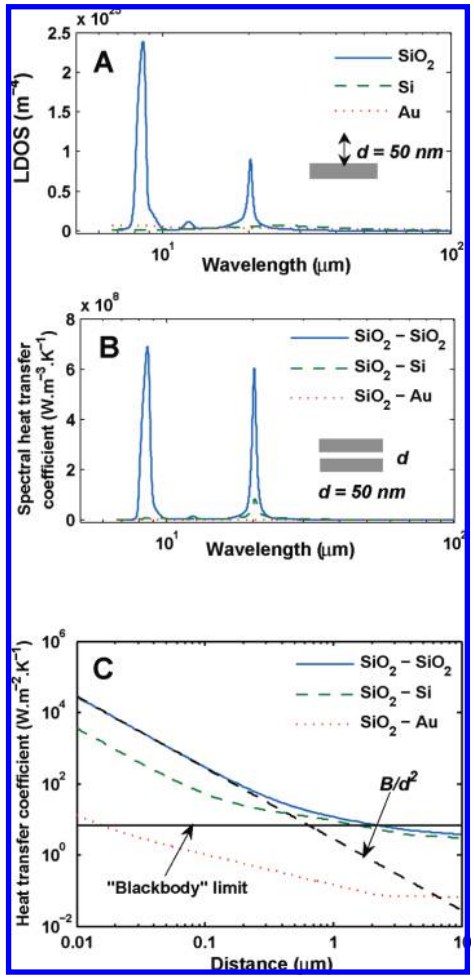

Figure 1. (A) Photon LDOS above an interface between vacuum and different materials at 50 nm. (B) Spectral radiative heat transfer coefficients for two parallel plates separated by a distance $d = 50$ nm at $T = 300$ K. (C) Radiative heat transfer coefficients versus the distance between two parallel plates at an average temperature $T = 300$ K. The black solid line is the limit of thermal radiation predicted by the blackbody radiation law, where the heat flux is calculated from Stefan−Boltzmann law as $\sigma(T_1^4 - T_2^4)$. The black dashed line is the asymptotic relation at small gaps (B/d^2).

SiO_2−Si, and SiO_2−Au). Resonant peaks similar to those seen in Figure 1A appear for the case of SiO_2−SiO_2 (Figure 1B), and thus the radiative heat transfer (Figure 1C) can be significantly enhanced at very small gaps. However, the radiation enhancement in the cases of SiO_2−Si and SiO_2−Au is much smaller because the mismatch of materials' properties between SiO_2 and Si or between SiO_2 and Au offset the resonance effects from a SiO_2 surface and results in a smaller enhancement (see Supporting Information).

In comparison with the extensive theoretical studies, only a few experiments were reported to measure thermal radiation between closely spaced bodies.[13−16] Experimentally it is very difficult to configure two parallel plates separated by nanoscale gaps and hence the several orders of magnitude increase by surface phonon polaritons in radiation exchange beyond Planck's blackbody radiation law as predicted in Figure 1 have not been demonstrated. We developed a sensitive technique to measure near-field radiative heat transfer between a microsphere and a substrate using a bimaterial

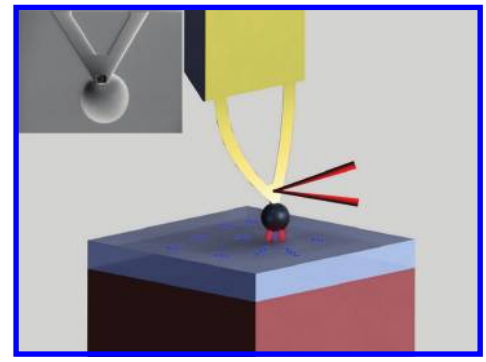

Figure 2. Schematic diagram of experimental setup. The thermal sensor is a silicon nitride AFM cantilever coated with a 70 nm gold film. A laser beam (650 nm wavelength, 3 mW output power) is focused on the tip of the cantilever and reflected onto a PSD. Application of voltage to the piezoelectric translation stage results in the movement of the substrate toward the sphere. In near-field, surface phonon polaritons can tunnel through the gap and they thus significantly contribute to the radiative heat transfer. The "cooling" effect on the cantilever due to the enhanced near-field radiation leads to the bending of the cantilever. Inset: A scanning electron microscope image of a glass sphere mounted on an AFM cantilever.

atomic force microscope (AFM) cantilever. A detailed description of our experimental setup has been given in a previous publication[17] and only key points are summarized here.

In Figure 2, a glass (silica) microsphere 50 or 100 μm in diameter is attached to the tip of a bimaterial (Si_3N_4/Au) AFM cantilever with UV adhesive. Silica spheres are chosen because of their availability in a wide range of diameters with good spherical shapes as well as their ability to support surface phonon polaritons. The output of the position sensing detector (PSD) is converted into an X or Y signal corresponding to the deflection of the AFM cantilever and a sum signal proportional to the incident laser power on it. A part of the laser power is absorbed by the gold film on the cantilever and thus creates a temperature rise on its tip and the sphere. The substrate and the supporting base of the cantilever are passively maintained at the ambient temperature. On the basis of the beam theory and the thermal analysis of a bimaterial AFM cantilever, we calibrate the cantilever and determine its effective thermal conductance between the laser spot and the base (7.91 μW•K^{-1}) and tip temperature (16.5 K higher than the ambient temperature at the given laser power) by measuring the bending of the cantilever in response to two different thermal inputs, power absorbed at the tip and ambient temperature.[18]

The substrate in Figure 2 is rigidly fixed to a piezoelectric motion controller that is able to reduce the gap between the sphere and the substrate below ~10 nm. The cantilever with the microsphere is oriented perpendicularly to the substrate to reduce the bending caused by Casimir and electrostatic forces during the experiment. When the system is pumped down to pressures less than 1×10^{-3} Pa, the heat conduction across the air gap between the sphere and the substrate can be neglected. Most of the laser power absorbed by the cantilever tip is transferred along the cantilever to its

supporting base, but a small amount (<0.5%) of absorbed heat is radiated to the surrounding (including the substrate) from the cantilever and the sphere. The deflection signal of the cantilever is linearly related to the heat transferred through the cantilever, where the proportional constant is determined by the properties and dimensions of the cantilever.[18] In the far-field where the gap between the sphere and the substrate is large, surface phonon polaritons are bound to the surfaces and cannot contribute to thermal radiation. Once the gap between the sphere and the substrate is small enough (Figure 2), the enhanced near-field radiation causes the cantilever to bend, responding to the change of temperature distribution in the cantilever due to the different thermal expansion coefficients of the two materials comprising the cantilever. The measured heat flux through the near-field radiation at small gaps is on the order of 100 nW, corresponding to a $\sim 10^{-2}$ K temperature change of the sphere. In the experiment, the far-field radiation loss from the sphere to the rest surrounding remains constant for a small sphere in a large enclosure,[19] where the large enclosure (vacuum chamber) is passively maintained at the ambient temperature. A $\sim 10^{-2}$ K temperature change of the sphere corresponds to ~1 nW change on the far-field radiation loss from the sphere, which is much smaller than the measured near-field radiative flux (~100 nW). Hence, our technique is sensitive to near-field radiation only.

In order to quantitatively measure and correct the force (Casimir and electrostatic forces) effects on our measurement, a very weak laser power is used to minimize the temperature difference between the sphere and the substrate (<1 K) and therefore the near-field radiation between them. Figure 3A shows the raw data measured under the laser light with different power leads for SiO_2-SiO_2. The blue curve is the typical near-field radiation signal measured under a high laser power. During the experiment, we use a piezosystem to change the gap between the sphere and the substrate and hold it constant for several seconds. When the substrate is held at a constant position, the deflection signal does not change and is seen as a "plateau". The jumps between two such plateaus are due to the change in the position of the substrate. The sharp change of the bending signal indicates the "contact" made between the sphere and the substrate, thereby providing a reference to determine the substrate−sphere separation distance. The green curve is the force signal under a weak laser power. In Figure 3A, when the cantilever is carefully oriented in a perpendicular manner to the substrate, the bending caused by the force is almost zero. At the steady state, the temperature of the microsphere is approximated as equal to the tip temperature of the cantilever because the radiation loss from the sphere is much smaller than the heat flow through the cantilever, considering that the conductance of the cantilever is much larger. Finally, the cantilever deflection signal measured by the PSD in Figure 3A, which is also linearly proportional to the heat transfer between the sphere and the substrate because the total absorbed laser power by the cantilever is a constant (corresponding to a constant sum signal of PSD during the experiment), is converted into heat transfer-distance curves.[17,18]

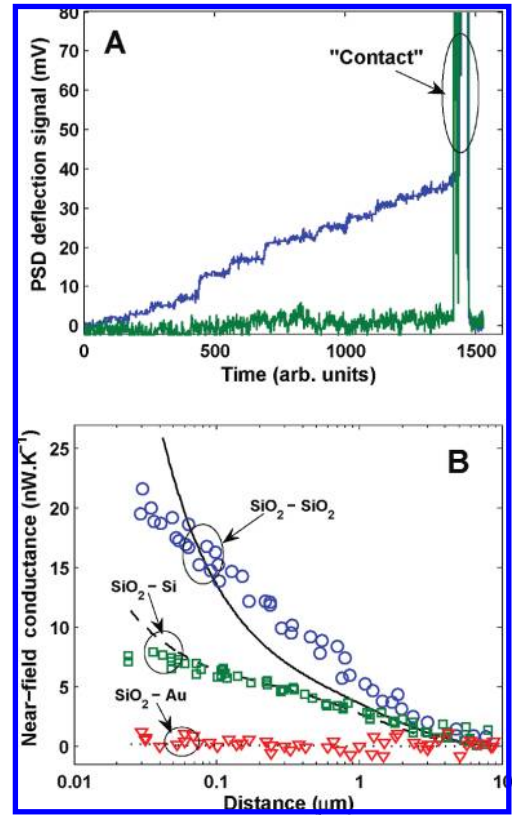

Figure 3. (A) The raw data measured under the laser light with two different power leads. The typical near-field radiation signal (blue curve) is measured under high laser power, where each plateau corresponds to a gap size. The force signal (green curve) is measured under weak laser power. The "contact" between the sphere and the substrate is manifested by the sharp change of the bending signal (PSD deflection signal). (B) Experimental data from the heat transfer−distance measurement and comparison with the theoretical prediction from the proximity force theorem (black curves). Each of the conductance data presented here is the averaged value of ~100 measurements with the standard deviation ~0.4 nW·K^{-1}. The experimental error on distance measurements is the resolution of the piezo system (~5 nm).

We tested the near-field signals between a glass sphere and each of the substrates considered (glass, doped silicon, and gold). The glass plate is a glass microscope slide. The silicon used in our work is n-type, arsenic doped with a carrier concentration of $\sim 2.6 \times 10^{19}$ cm^{-3} measured using the Hall effect technique. The optical constants of the doped silicon are calculated from the models in ref 7. The metal plate is fabricated by coating a 1 μm thick gold film on a glass slide. The skin depth of gold in the infrared range is estimated to be ~15 nm so that 1 μm thick gold film is sufficient to neglect the effect from the glass slide underneath it. All the substrates are rinsed with isopropanol and are blown dry with nitrogen before testing. In Figure 3B, the measured near-field radiative heat conductance, defined as the heat transfer divided by the temperature difference, is plotted as a function of the gap between the sphere and the substrates. Using an AFM we measure the average surface roughness amplitude of three surfaces as 3.3 nm for glass, 3.9 nm for silicon, and 3.4 nm for gold. The gap size ranges from ~30 nm to 10 μm, considering the surface roughness and the resolution of piezoelectric motion system. The effect

of surface phonon polaritons is clearly shown in Figure 3B, where we see that near-field radiation is strongly enhanced when the sphere and the substrate are both made of polar dielectric materials. Compared to our previous publication (ref 17), we used a piezosystem to precisely control the gap with high resolution, which leads to much less scatter in the experimental data. We also pushed the gap down to ~30 nm and studied different materials (metal and semiconductor) so that clear conclusion can be drawn on surface wave contributions.

There is no rigorous theoretical calculation for the near-field radiation between a microsphere and a plate because of computational difficulties. A similar situation occurs in the Casimir force measurement.[20,21] So, for the sphere−plate geometry, the near-field radiation is estimated by the so-called proximity force theorem[22] that approximates curved surfaces by differential flat areas and using the known solutions for near-field radiation between parallel surfaces to obtain the sphere−plate near-field radiative conductance,

$$G_{\text{near-field}}^{\text{sphere-plate}}(d) \cong 2\pi R \int_{s=d}^{\infty} h_{\text{near-field}}^{\text{plate-plate}}(s)ds \qquad (1)$$

where G is the near-field conductance, h is the heat transfer coefficient, and R is the radius of the sphere. We see from Figure 1C that the heat transfer coefficient between two glass surfaces follows an asymptotic relation given by $h \approx B/d^2$, where B is constant and d is gap distance. At small gaps, eq 1 can be further simplified as $G_{\text{near-field}}^{\text{sphere-plate}}(d) \cong 2\pi Rd(B/d^2)$. The above relation for near-field conductance between a sphere and a flat surface can also be interpreted as the near-field conductance between two flat surfaces of area $2\pi Rd$ or a disk of radius $(2Rd)^{1/2}$. In Figure 3B, the calculated conductance-distance (black curves) from eq 1 is compared with our experimental data. In general, the proximity theory gives a correct order of magnitude in the experimental range and is in reasonable agreement with experimental results. The discrepancies between experiment and proximity theory in Figure 3B for SiO_2-SiO_2 shows that the proximity approximation is not entirely valid for the near-field radiation between a sphere and a plate because of significant mathematical simplifications, consistent with our previous theoretical studies.[23] Because of the large ratio of relevant length scales of the problem (nanometer size gap, tens of micrometers of sphere radius, and zero radius of curvature of the flat plate), however, no exact numerical solution can be obtained for the sphere−plate problem so far and detailed mechanisms for the discrepancy between experiments and the proximity theory calculation should be investigated in future studies. The reason for the better agreement between experiment and theory for Si and Au surfaces may be that the near-field radiation for SiO_2-Si or SiO_2-Au increases less rapidly with decreasing gap distances than for that between SiO_2-SiO_2 (Figure 1C). Hence, to some extent, the above issues discussed for SiO_2-SiO_2 are mitigated for SiO_2-Si and SiO_2-Au.

It is well known that nonresonant evanescent waves can also contribute to near-field radiation for any material.[6] However, for the near-field radiation between polar dielectric materials, the contribution from resonant surface waves is dominant and much larger than that from nonresonant evanescent waves (see Supporting Information). In the present sphere−plate experimental system, only a small fraction of the sphere area contributes to the near-field radiation transfer between the sphere and the plate. A direct comparison of the conductance of the near-field radiation to that of a blackbody, treating the whole sphere as a blackbody, is hence not appropriate. It was mentioned earlier that the near-field radiation between a sphere and a flat surface can be interpreted as near-field radiation between two parallel planar surfaces of area $2\pi Rd$. When normalized to this equivalent area, the near-field radiative heat transfer coefficient in SiO_2-SiO_2 is ~ 2230 $W\cdot m^{-2}\cdot K^{-1}$ at a ~30 nm gap, compared to ~ 3.8 $W\cdot m^{-2}\cdot K^{-1}$ for blackbody radiation (Figure 4). This is the first time, to our knowledge, the near-field radiation mediated by resonant surface phonon polaritons is observed to exceed the blackbody radiation limit by 3 orders of magnitude at nanoscale gaps. In the same figure, we also plotted the near-field portion of the radiation heat transfer coefficient between two parallel plates (dashed curves) after subtracting the far field contribution. The magnitude of the sphere−plate heat transfer coefficient compares well with that between two parallel plates. However, the discrepancies between the two are also clear and consistent with our discussions earlier.

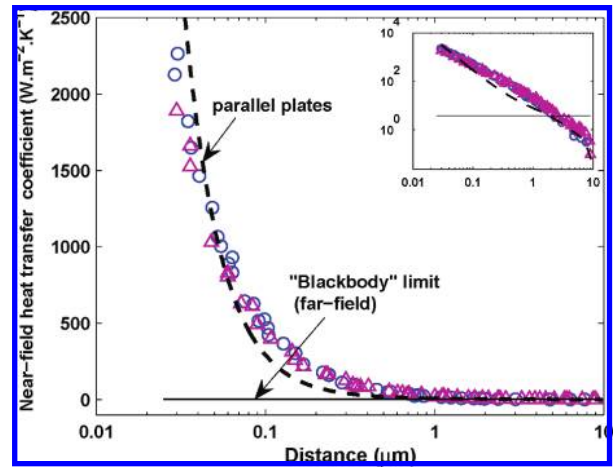

Figure 4. Equivalent sphere−plate near-field heat transfer coefficients normalized to the area $2\pi Rd$ versus the gap distance for a 100 μm (blue circles) and a 50 μm (violet triangles) diameter sphere. The flat line is the limit predicted by Planck's blackbody radiation law. The dashed line is the near-field heat transfer coefficients obtained after subtracting the far-field part taken from Figure 1C. Inset: the plot on a log−log scale.

In summary, our experimental demonstration of the extremely high radiative heat transfer between polar dielectric surfaces at nanometer gaps, exceeding by 3 orders of magnitude the predictions of Planck's blackbody radiation law, may bring new opportunities to fundamental and applied research on radiative cooling and thermophotovoltaic technologies. Near-field radiation is also important for the thermal management of magnetic heads in data storage, heat-assisted data storage, and other microelectromechanical devices. The experimental work presented here can also shed light on the thermal contributions to the Casimir force.

Acknowledgment. The authors thank Mr. A. Henry for preparing the manuscript and Mr. J. Tong for helping with schematic drawings of experimental setup. This work is supported by DOE (DE-FG02-02ER45977) and AFOSR MURI through UIUC.

Supporting Information Available: This material is available free of charge via the Internet at http://pubs.acs.org.

References

(1) Planck, M. *The Theory of Heat Radiation*; Dover: New York, 1959.
(2) Rytov, S. M. *Theory of Electric Fluctuations and Thermal Radiation*; Air Force Cambridge Research Center: Bedford, MA, 1959.
(3) Polder, D.; Van Hove, M. *Phys. Rev. B* **1971**, *4*, 3303.
(4) Mulet, J. P.; Joulain, K.; Carminati, R.; Greffet, J. J. *Microscale Thermophys. Eng.* **2002**, *6*, 209.
(5) Volokitin, A. I.; Persson, B. N. *Rev. Mod. Phys.* **2007**, *79*, 1291.
(6) Pendry, J. B. *J. Phys.: Condens. Matter* **1999**, *11*, 6621.
(7) Fu, C. J.; Zhang, Z. M. *Int. J. Heat Mass Transfer* **2006**, *49*, 1703.
(8) Barnes, J. R.; Stephenson, R. J.; Welland, M. E.; Gerber, C.; Gimzewski, J. K. *Nature* **1994**, *372*, 79.
(9) Majumdar, A. *Annu. Rev. Mater. Sci.* **1999**, *29*, 505.
(10) Greffet, J. J.; et al. *Nature* **2002**, *416*, 61.
(11) Hillenbrand, R.; Taubner, T.; Keilmann, F. *Nature* **2002**, *418*, 159.
(12) Joulain, K.; Carminati, R.; Mulet, J. P.; Greffet, J. J. *Phys. Rev. B* **2003**, *68*, 245405.
(13) Domoto, G. A.; Boehm, R. F.; Tien, C. L. *J. Heat Transfer* **1970**, *92*, 412.
(14) Hargreaves, C. M. *Philips. Res. Rep. Suppl.* **1973**, *5*, 1.
(15) Xu, J. B.; Lauger, K.; Moller, R.; Dransfeld, K.; Wilson, I. H. *J. Appl. Phys.* **1994**, *76*, 7209.
(16) Kittel, A.; et al. *Phys. Rev. Lett.* **2005**, *95*, 224301.
(17) Narayanaswamy, A.; Shen, S.; Chen, G. *Phys. Rev. B* **2008**, *78*, 115303.
(18) Shen, S.; Narayanaswamy, A.; Goh, S.; Chen, G. *Appl. Phys. Lett.* **2008**, *92*, 63509.
(19) Siegel, R.; Howell, J. *Thermal Radiation Heat Transfer*; Taylor and Francis: New York, 2002.
(20) Mohideen, U.; Roy, A. *Phys. Rev. Lett.* **1998**, *81*, 4549.
(21) Munday, J. N.; Capasso, F; Adrian Parsegian, V. *Nature* **2009**, *457*, 170.
(22) Blocki, J.; Randrup, J.; Swiatecki, W. J.; Tsang, C. F. *Ann. Phys.* **1977**, *105*, 427.
(23) Narayanaswamy, A.; Chen, G. *Phy. Rev. B* **2008**, *77*, 075125.

NL901208V